C. R. Mecanique 347 (2019) 305–317

Contents lists available at ScienceDirect

Comptes Rendus Mecanique

www.sciencedirect.com

Patterns and dynamics: homage to Pierre Coullet / *Formes et dynamique : hommage à Pierre Coullet*

Limiting speed for jumping

Une vitesse limite pour le saut

Mary Carmen Jarur [a,*], Jacques Dumais [b], Sergio Rica [c]

[a] *Universidad Católica del Maule, Talca, Chile*
[b] *Facultad de Ingeniería y Ciencias, Universidad Adolfo Ibáñez, Avda. Padre Hurtado 750, Viña del Mar, Chile*
[c] *Facultad de Ingeniería y Ciencias and UAI Physics Center, Universidad Adolfo Ibáñez, Avda. Diagonal las Torres 2640, Peñalolén, Santiago, Chile*

ARTICLE INFO

Article history:
Received 18 October 2018
Accepted 17 December 2018
Available online 2 April 2019

Keywords:
Jumping
Take-off velocity
Locomotion
Limiting speed
Biomechanics

Mots-clés :
Saut
Vitesse de décollage
Locomotion
Biomécanique

ABSTRACT

General mechanical considerations provide an upper bound for the take-off velocity of any jumper, animate or inanimate, rigid or soft body, animal or vegetal. The take-off velocity is driven by the ratio of released energy to body mass. Further, the mean reaction force on a rigid platform during push-off is inversely proportional to the characteristic size of the jumper. These general considerations are illustrated in the context of Alexander's jumper model, which can be solved exactly and which shows an excellent agreement with the mechanical results.

RÉSUMÉ

Des considérations mécaniques générales fournissent une limite supérieure pour la vitesse de décollage de tout sauteur, qu'il soit animé ou inanimé, qu'il soit de corps rigide ou mou, animal ou végétal. La vitesse de décollage est déterminée par le rapport entre l'énergie libérée et la masse corporelle. De plus, la force de réaction moyenne sur un support rigide lors du *push-off* est inversement proportionnelle à la taille caractéristique du sauteur. Ces considérations générales sont illustrées à l'aide du modèle de saut d'Alexander, qui peut être résolu exactement et qui offre un excellent accord avec les résultats mécaniques.

1. Introduction

Jumping in animals such as insects and vertebrates is restricted by a take-off speed limit of about 6 m/s for a broad range of species of various body shapes and masses. This observation goes back to the 17th century and it is known as Borelli's law: "the take-off velocity is almost independent of the body mass" [1]. Moreover, the existence of such limiting speed

* Corresponding author.
E-mail addresses: mjarur@ucm.cl (M.C. Jarur), jacques.dumais@uai.cl (J. Dumais), sergio.rica@uai.cl (S. Rica).

https://doi.org/10.1016/j.crme.2019.03.005
1631-0721/

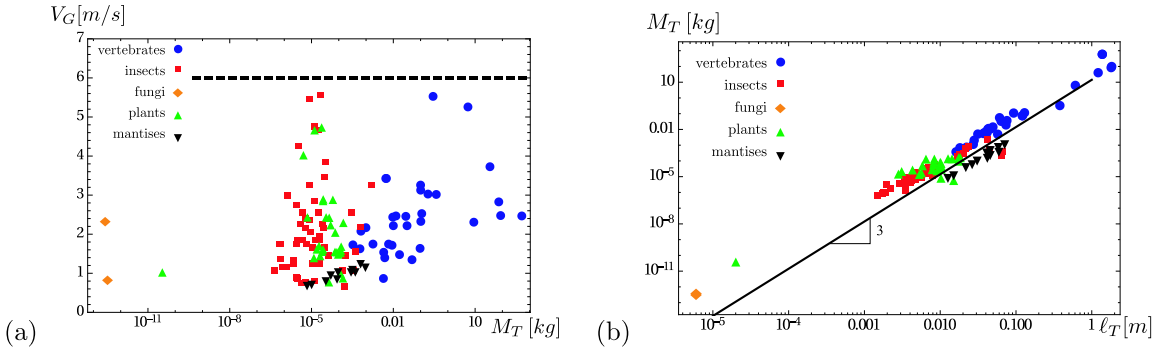

Fig. 1. (a) Take-off velocities for vertebrates, invertebrates, plants, and fungi of various masses. The black triangles plot the observations of Ref. [5] on different body-size mantises. (b) Body-length vs body-mass plot, showing an approximative relation, $M_{\mathrm{T}} \approx \varrho\, \ell_{\mathrm{T}}^3$ with $\varrho \approx 14.2$ [kg/m^3], represented by the black line.

does not depend on the vertebrate or invertebrate character of the animal. This observation can be extended to the world of plants and fungi, which have developed jumping mechanisms for seed and spore release [2,3], as well as to mechanical engines [4].

Fig. 1a compiles the take-off velocity for a large number of species, including vertebrates, invertebrates, plants, and fungi. As can be seen, none of the jumpers exceeds a take-off velocity of 6 m/s, despite the jumpers' masses varying over a range of 15 orders of magnitude, *i.e.* from 10^{-12} kg up to 10^3 kg. Moreover, at this scale, it is difficult to infer any specific law relating body mass and take-off velocity, because there exist large variations of the take-off velocity for a particular body mass. Therefore we focus our attention on the existence of a limiting speed which appears to be independent of body mass or the size of the extremity. Additionally to the take-off velocity body-mass relation, Fig. 1b shows the characteristic length of the jumper as a function of the body mass. This shows a clear relation of the type $M_{\mathrm{T}} \sim \ell_{\mathrm{T}}^3$ (hereafter, we denote M_{T} and ℓ_{T} the total mass and length of the body). The existence of a mass–length relation $M_{\mathrm{T}} \approx \varrho\, \ell_{\mathrm{T}}^3$ over a large number of decades reveals that most living organisms have approximately the same density (close to the density of water). However, notice that the similarity law observed in Fig. 1b displays a large band of dispersion (about two decades in the transverse direction) because of shape variations.

Jumping in vertebrates has been studied by modeling a body trunk together with articulated leg segments. These leg segments are coupled with simple constitutive equations for muscular activity [6–8]. A simple model consisting of a trunk, two legs, and a Hill-type musculature was introduced by Alexander [9]. This model was applied to humans, bushbabies, and locusts; and it considered three types of jumping techniques: catapult, squat jump, and countermovement. Alexander confirmed the advantage of each one of these distinct jumping strategies such as catapult for insects and countermovement for humans. Although Alexander's model lacks anatomical specificity, its simplicity is an advantage, because it can be solved analytically.

A more detailed human model taking into account the optimal muscular distribution in the legs was introduced by Wong et al. [8]. This model highlights the muscle cross-sectional areas as an essential parameter for improving jumping performance and it allows quantitative predictions for the contribution of specific muscle groups in the leg. However, we focus on the simplicity of Alexander's model, not only because it is analytically trackable, but also because the model predicts performance levels that are in good agreement with empirical data [10].

In contrast recent publications have modeled jumping using robots [11] with a mechanism composed of an actuated mass-spring system showing the importance of the resonance for the spring system. In this situation the actuator provides energy via an additive sinusoidal forcing, therefore it should be considered as a dissipative system. In this situation, an energy-dissipation balance governs the jump. This kind of jump will not be studied in this paper.

Other jumping studies consider the factors that may limit the jumping performance, and they are focused on energy available and power requirement per unit mass [5,12,13] fundamentally, aspects that we will discuss later. But the question about the limit is not facing directly.

In this paper, we derive, in Section 2, a general take-off condition regarding the energy of the center of mass valid under some assumptions discussed below, for both conservative or dissipative jumps. This condition tells us that, at take-off, the center of mass energy reaches a maximum. Similarly, the take-off velocity of the center of mass is bounded, for both conservative and dissipative systems, from above by (see Eq. (4) below) the muscular energy per unit mass, hereafter U_m^*. As in the case of the mass–length relation, the muscular energy per unit mass, U_m^*, is roughly a constant number because it concerns the intrinsic properties of the bio-materials composing muscles, tendons, etc. Therefore, the apparently non-dependence of the take-off velocity on the body mass appears to be a consequence of the hypothesis that the stored muscular energy ΔU_{m} (defined below) provided for jumping is proportional to the body mass. This is essentially the hypothesis behind Borelli's law [14]. In the same line, we derive a relation for the mean ground reaction force with a dependency inversely proportional to the body length size (see Fig. 2). In Section 3, we illustrate these relations for Alexander's model for a jumper, whereas

the calculations can be performed exactly. Then, in section 3.2, we evaluate the take-off velocity, as well as the push-off normal reaction force, both as a function of different parameters of the model.

2. Mechanical considerations

2.1. Dynamics of the center of mass

Jumping of an animate or inanimate, rigid or soft body, can be considered a classical mechanical problem involving a large number of interconnected parts subjected to internal and external forces that may be conservative or not. Although the application of Newtonian mechanics can be quite complex, because of the third law, the motion of the center of mass does not involve any internal forces (neither conservative nor dissipative). Newton's law for the center of mass dictates (below $\hat{\boldsymbol{z}}$ is the vertical unitary vector pointing upward):

$$M_{\mathrm{T}}\frac{\mathrm{d}\boldsymbol{v}_G}{\mathrm{d}t} = -M_{\mathrm{T}}g\hat{\boldsymbol{z}} + \boldsymbol{F}_{\mathrm{ext}} \tag{1}$$

where M_{T} is the total mass of the body, $\boldsymbol{v}_{\mathrm{G}}(t)$ is the velocity vector of the center of mass, $-M_{\mathrm{T}}g\hat{\boldsymbol{z}}$ is the total weight, and $\boldsymbol{F}_{\mathrm{ext}}$ represents all external forces acting on the body other than weight. In what follows, we assume that all external forces are purely of contact type, *i.e.* we discard the effect of air resistance and other external forces. In a jump, these contact forces vanish at the point of take-off. Thereafter, regardless of internal motions, the center of mass follows a pure ballistic trajectory. Then, in this context Eq. (1) plays a central role in the push-off jump phase as we will see next.

2.2. The center of mass energy

In the process of jumping, the various external and internal forces transform the involved energies into mechanical energy of the center of mass, which is the relevant energy for the jump, as we show in what it follows. The maximum height reached by a jumper depends only on the center of mass energy at take-off (assuming a purely vertical jump).

The mechanical energy, $E = K + U$, includes a kinetic energy term, K, and the potential energy U that comes from the conservative forces involved in the problem.

We denote by K_{G} the kinetic energy of the center of mass of the system and by K_r the relative kinetic energy with respect to the center of mass. Therefore, by König's theorem, the total kinetic energy splits into $K = K_{\mathrm{G}} + K_r$ (both positive). Contrarily, the potential energy U contains two contributions: the gravitational energy of the center of mass (the weight), U_{G}, and all internal energies of muscular origin, U_{m}, hence $U = U_G + U_{\mathrm{m}}$. Finally, the total mechanical energy reads $E = E_{\mathrm{G}} + E_r$ with $E_{\mathrm{G}} = K_{\mathrm{G}} + U_{\mathrm{G}}$ and $E_r = K_r + U_{\mathrm{m}}$. Nevertheless, for jumping, the mechanical energy of the center of mass reads simply

$$E_{\mathrm{G}} = \frac{1}{2}M_{\mathrm{T}}|\boldsymbol{v}_{\mathrm{G}}|^2 + M_{\mathrm{T}}gz_{\mathrm{G}} \tag{2}$$

where z_G is the height of the center of mass. Even in the case of pure conservative forces, this energy is not conserved, since:

$$\frac{\mathrm{d}}{\mathrm{d}t}E_{\mathrm{G}} = M_{\mathrm{T}}\boldsymbol{v}_{\mathrm{G}}\cdot\frac{\mathrm{d}\boldsymbol{v}_{\mathrm{G}}}{\mathrm{d}t} + M_{\mathrm{T}}g\boldsymbol{v}_{\mathrm{G}}\cdot\hat{\boldsymbol{z}} = \boldsymbol{v}_{\mathrm{G}}\cdot\boldsymbol{F}_{\mathrm{ext}} \tag{3}$$

In (3), we have used explicitly Eq. (1).

Therefore, one concludes that, at take-off ($\boldsymbol{F}_{\mathrm{ext}} = 0$), the mechanical energy of the center of mass reaches its maximum at $t = t_{\mathrm{c}}$, that is $\mathrm{d}E_{\mathrm{G}}/\mathrm{d}t|_{t=t_{\mathrm{c}}} = 0$.[1]

2.3. General bound for the take-off velocity

2.3.1. Conservative jump

In the case of a conservative jump, the total energy is conserved during the push-off phase,

$$E = \frac{1}{2}M_{\mathrm{T}}|\boldsymbol{v}_{\mathrm{G}}|^2 + M_{\mathrm{T}}gz_{\mathrm{G}} + K_r + U_{\mathrm{m}} = M_{\mathrm{T}}gz_{\mathrm{G}}(0) + U_{\mathrm{m}}(0)$$

and the above energy is equal to its initial value at rest ($\boldsymbol{v}_{\mathrm{G}}(0) = 0$ and $K_r = 0$), and $z_{\mathrm{G}}(0)$ being the initial position of the center of mass and $U_{\mathrm{m}}(0)$ the initial muscular stored energy.

[1] This statement is a generalization of the Tait–Thomsom theorems [W. Thomson and P. Tait, Treatise on Natural Philosophy, Oxford University Press, 1888], §311: *"Given any material system at rest, and subjected to an impulse of any magnitude and in any specific direction, it will move off so as to take the greatest amount of kinetic energy which the specified impulse can give it."* and §312: *"Given any material system at rest. Let any parts of it be set in motions suddenly with given velocities, the other parts being influenced only by their connections with those which are set in motion, the whole system will move so as to have less kinetic energy than belongs to any other motion fulfilling the given velocity conditions."*

At take-off, $t = t_c$, the take-off velocity becomes $V_G = |\boldsymbol{v}_G(t_c)|$, and:

$$\frac{1}{2}M_T V_G^2 = \Delta U_m - M_T g\,(z_G(t_c) - z_G(0)) - K_r$$

where $\Delta U_m = U_m(0) - U_m(t_c) \geq 0$. This quantity is necessarily positive in the case of a jump. Moreover, we shall assume that a jump also satisfies the inequality $z_G(t_c) \geq z_G(0)$, that is, there is a body expansion increasing the center of mass height during the push-off phase. Therefore, because the relative kinetic energy is always positive ($K_r \geq 0$), one then concludes that the center of mass take-off velocity is upper bounded by

$$V_G \leq \sqrt{\frac{2\Delta U_m}{M_T}} = \sqrt{2U_m^*} \tag{4}$$

where $U_m^* = \frac{\Delta U_m}{M_T}$ is the muscular energy per unit mass.

2.3.2. Dissipative jump

The same inequality (4) holds for a dissipative jump, indeed the energy variation is related to the work done by all the dissipative forces, denoted by $R \geq 0$, thus

$$\Delta E = \frac{1}{2}M_T V_G^2 + M_T g z_G(t_c) + K_r + U_m(t_c) - (M_T g z_G(0) + U_m(0)) = -R \leq 0$$

Therefore, under the same conditions as in the conservative case and in addition to the dissipative character of muscular forces (heat for instance, fatigue, irreversibility, etc., $R < 0$), one gets the same upper bound (4).

2.4. Mean reaction force

We turn now to the variation of the normal reaction during the push-off phase. The explicit temporal variation of the reaction force is readily obtained by knowing the acceleration of the center of mass and using Eq. (1). However, in general it is not possible to obtain this acceleration without knowing the motion of all parts, therefore we shall consider just the mean value. The integration in time of the vertical component of Eq. (1) during the push-off phase reads:

$$M_T \int_0^{t_c} \frac{\mathrm{d}v_G}{\mathrm{d}t}\,\mathrm{d}t = M_T V_G = -M_T g t_c + \int_0^{t_c} F_N(t) u \mathrm{d}t$$

therefore

$$\langle F_N \rangle = \frac{1}{t_c}\int_0^{t_c} F_N(t)\mathrm{d}t = M_T g + \frac{M_T V_G}{t_c}$$

In consequence, the mean reaction force per weight becomes

$$\frac{\langle F_N \rangle}{M_T g} - 1 = \frac{V_G}{g t_c} \tag{5}$$

The reaction time, t_c, remains unknown and in general it depends on the motion of all parts. However, it may be estimated, assuming that the accelerated motion of the center of mass experiences a displacement in an amount of the order of an extremity size, s (which is of the order of ℓ_T), hence $s \approx \frac{1}{2}a t_c^2 \approx \frac{1}{2}V_G t_c$, and consequently the mean normal force must follows a scaling relation of the type:

$$\frac{\langle F_N \rangle}{M_T g} - 1 \approx \frac{V_G^2}{2gs} \tag{6}$$

Because the take-off velocity is bounded, it is expected that the normal force may satisfy:

$$\frac{\langle F_N \rangle}{M_T g} - 1 \sim \frac{\Delta U_m}{M_T g \ell_T} \tag{7}$$

In conclusion, for smaller body sizes, the quotient reaction-force weight is greater. Indeed, for instance, for humans the reaction force is three times the body weight, the galago's reaction force is 12 times its weight, 58 times for locusts, and 135 in the case of fleas. This tendency is compared with the available data used in Fig. 1 (and spanned over five decades) in the next Fig. 2. A similar plot was published by Vogel [14], including both jumper and biological projectiles showing the inverse proportionality to the body-size observed scaling. Vogel [14] explains that this scaling is related to the fact that

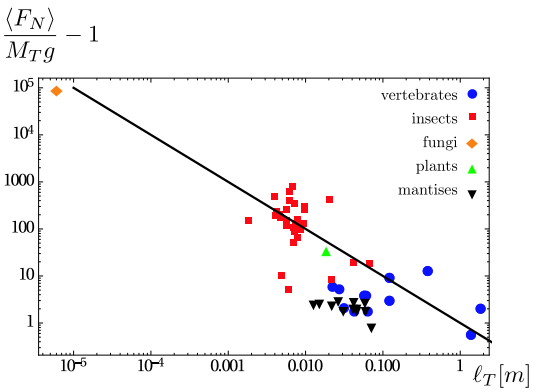

Fig. 2. Mean reaction force $\langle F_N \rangle / (M_T g) - 1$ during take-off as a function of ℓ_T for the case of vertebrates, invertebrates, plants, and fungi of various organisms used in Fig. 7. The line corresponds to the scaling $1/\ell_T$. For the purpose of comparison, we added explicitly the case of biological projectiles provided by Vogel [14].

the push-off force is proportional to the area of the muscular cross section, thus the force–weight ratio becomes inversely proportional to a length.

Despite the excellent agreement displayed in Fig. 2, we must remark the fact that equations (6) and (7) are, yet, not rigorous results as it is inequality (4).

2.5. Discussion

The general character of the previous results implies the validity of them for any configuration, let it concern vertebrates or invertebrates or a robot jumping on a rigid planform. The situation becomes different in the case of plants in which a seed (that is a projectile) is launched from a mobile planform that recoils at take-off. Nevertheless, in the later case, the energy lost by the recoiled planform ensures the validity of the general bound (4).[2]

Undoubtedly, living organism are far from being a conservative system; however, the take-off condition (3) as well as the upper bound for the take-off velocity (4) does not depend on the conservative nor the dissipative character of the muscular forces.

Contrarily, a purely conservative system has the advantage of being analytically tractable for most of the relevant calculations. On the other hand, because dissipative effects imply loss of energy, it appears naturally that the conservative case provides a correct upper bound for performance, that is, a value for the maximum take-off velocity. Therefore, the conservative case does not appear to be only a mathematical solvable case, but also a good upper bound for the limiting speed. More importantly, there are some examples in nature where the initial stored energy and the jump performance are best interpreted as a conservative process (*e.g.*, insects employing catapult mechanisms [15]). Indeed, an energy conservation assumption is justified by experimental observations of existing records regarding the jumping performance in frogs [16,17] as well as in galagos [18].

For the above reasons, in the following sections, we restrict our analysis to a purely conservative scenario.

3. Application to Alexander's model [9]

3.1. The model

The original model proposed by Alexander [9] consists in a symmetrical jumper composed of a trunk and two legs. The legs are formed by two segments of length s, which scales as ℓ_T. The trunk mass is m_1, being m_2 and m_3 the leg's masses (see Fig. 3). Each leg segment forms an angle (2θ) at the knee. We emphasize that the angles of the thigh (proximal segment labeled by 2) and the lower limb (distal segment labeled by 3) with respect to the horizontal plane are the same because of a non-slide geometrical constraint at the contact points with the ground. Assuming that these segments have different lengths, then a "no-sliding" condition implies a geometrical constraint on the knee angles, which complicates the mathematical analysis, but actually without any relevant consequences. Finally, the torque T exerted by each knee provides the energy for the jump, starting from a position of rest $(2\theta_0)$. As noted by Alexander, we can remark that an explicit dependence of the knee torque on the flexion angle is not crucial. Therefore, we consider roughly a constant torque $T = -\frac{\partial U_m}{\partial \theta} \approx$ constant. Although this model is oversimplified, the jumper has the advantage of being described by a single variable, $\theta(t)$, and can therefore be solved analytically.

[2] We remark an exception, namely the case where the take-off position of the center of mass is lower than the original one, $z_G(t_c) < z_G(0)$. That case should be investigated separately.

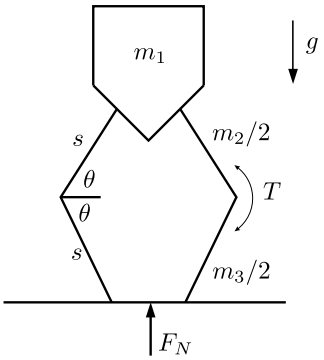

Fig. 3. Scheme for the two-segment model. The total leg length is $2s$ and the total body mass is $M_T = m_1 + m_2 + m_3$, T is the torque exerted at each knee, and F_N is the ground reaction force, *e.g.*, the normal force.

This model is solved using the usual tools of classical mechanics. The mechanical energy reads (see Appendix 5.1):

$$E = \frac{1}{2} I_2(\theta)\dot{\theta}^2 + \frac{1}{2} g\delta_2 \sin\theta - 4T\left(\theta - \frac{\pi}{2}\right) \tag{8}$$

where, we define, as a short-hand notation,

$$I_2(\theta) = s^2\left[\frac{1}{3}(m_2 + m_3) + 2(2m_1 + m_2)\cos^2\theta\right] \tag{9}$$

$$\delta_2 = s(4m_1 + 3m_2 + m_3) \tag{10}$$

Notice that, because of the previous convention, we define the zero muscular energy by the energy at the non-elongated configuration ($\theta = \pi/2$). Alexander's model describes the situation of a conservative motion, hence the energy (8) is constant, and it may be computed in terms of the initial conditions, $\theta(t=0) = \theta_0$ and $\dot{\theta}(t=0) = 0$. Therefore, the mechanical energy (8) provides us with a first integral of motion, which allows us to compute $\theta(t)$. The final result is obtained after integrating the following first-order differential equation:

$$\dot{\theta}^2 = \frac{1}{I_2(\theta)}\left[8T(\theta - \theta_0) - g\delta_2(\sin\theta - \sin\theta_0)\right] \tag{11}$$

Here we make the identification $\Delta U_{\mathrm{m}}(\theta) = 4T(\theta - \theta_0)$. Equation (11) provides an explicit solution for the angle θ as a function of time. Although it cannot be written in terms of elementary functions, it can be formally integrated.

Additionally, the take-off condition requires the knowledge of the vertical velocity of the center of mass, which is given by the relation:

$$v_{\mathrm{G}} = \frac{1}{2}\frac{\delta_2}{M_{\mathrm{T}}}\cos\theta\,\dot{\theta} \tag{12}$$

where the total mass is $M_{\mathrm{T}} = m_1 + m_2 + m_3$. Hence, Eq. (1) allows us to write:

$$M_{\mathrm{T}}\frac{\mathrm{d}v_{\mathrm{G}}}{\mathrm{d}t} = \frac{\delta_2}{2}(\cos\theta\ddot{\theta} - \sin\theta\dot{\theta}^2) = -M_{\mathrm{T}}g + F_{\mathrm{N}}$$

Therefore, the contact force in terms of the dynamical variables becomes:

$$F_{\mathrm{N}} = M_{\mathrm{T}}g + \frac{\delta_2}{2}(\cos\theta\ddot{\theta} - \sin\theta\dot{\theta}^2) \tag{13}$$

which may be written explicitly in terms of the angular variable, θ, after using (11) and its derivative. (See Eq. (31) in Appendix 5.2.)

Further, the take-off condition imposes $F_{\mathrm{N}} = 0$ and provides an equation for the critical take-off angle θ_{c}. (See Eq. (32) in Appendix 5.2.) Because these conditions involve a mixture of polynomial and trigonometric functions, *i.e.* a transcendental equation, it can be solved only numerically by assigning different parameter values to it. After computing, the take-off angle θ_{c}, the take-off angular velocity $\dot{\theta}_{\mathrm{c}}$, the velocity of the center of mass, and the normal force can all be calculated in a fairly straightforward way as functions of the model parameters (m_1, m_2, m_3, s, g, and T). The jump take-off velocity of the center of mass (12) becomes:

$$V_G = v_{\mathrm{G}}(t_{\mathrm{c}}) = \frac{1}{2}\frac{\delta_2}{M_{\mathrm{T}}}\cos\theta_{\mathrm{c}}\dot{\theta}_{\mathrm{c}} \tag{14}$$

In the same way, we can compute the maximum value of the normal force (13).

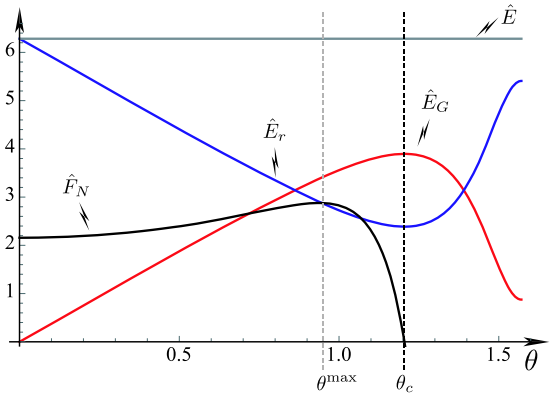

Fig. 4. Dimensionless partial energies and reaction force as a function of the flexion angle θ for the two-segment model. The plot includes the total energy $\hat{E} = E/T$ (all energies are normalized by T), which is constant for all angles (gray line). We also plot the energy of the center of mass labeled by $\hat{E}_G$ (red curve) and the internal energy $\hat{E}_r$ (blue line). Lastly, we plot the normalized force $\hat{F}_N = F_N s/T$ (black curve). Notice that, as explained in the main text, the take-off condition, θ_c, arises at the maximum of $\hat{E}_G$ (and consequently, because of energy conservation, as the minimum of $\hat{E}_r$), and it coincides with the condition $\hat{F}_N = 0$. We also mark the location of the maximum reaction force just before take-off, $\theta^{\max}$. In the plot, we consider the parameter values: $m_1/M_T = 0.7$, $m_2/M_T = 0.2$, and $m_3/M_T = 0.1$, $\theta_0 = 0$ and $T/(M_T g s) = 2$.

3.2. Take-off velocity and reaction force for the two-segment model

3.2.1. Dimensional analysis

Alexander's model depends upon the following parameters:

$$M_T,\ m_2,\ m_3,\ s,\ T,\ \text{and}\ g$$

corresponding to the total body mass, the tight and lower limb masses and lengths, the knee torque and gravity, respectively. From this set of six parameters, we can define three dimensionless quantities:

$$\mu_2 = \frac{m_2}{M_T},\ \mu_3 = \frac{m_3}{M_T},\quad \text{and}\quad \tau = \frac{T}{M_T g s} \tag{15}$$

In the following, the jump velocity V_G, the normal force F_N, and the energies will be re-scaled by the dimensionless quantities:

$$\hat{V}_G = \frac{V_G}{\sqrt{T/M_T}},\quad \hat{F}_N = \frac{F_N s}{T},\quad \text{and}\quad \hat{E} = \frac{E}{T}$$

which are the relevant dimensionless observables fully characterizing the current jumping model.[3]

3.2.2. General integration of the equation of motion

Based on the exact solution given by Eq. (11), we can compute the different energy contributions involved in Eq. (8), as well as the normal reaction (13) (or Eq. (31) in Appendix 5.2) in terms of the angular variable θ without any knowledge of the take-of timef. Fig. 4 plots the evolution of the dimensionless energy of the center of mass, $\hat{E}_G$, the internal dimensionless energy, $\hat{E}_r$, and the dimensionless reaction force, $\hat{F}_N$, as a function of the flexion angle θ, for the two-segment model. As it can be seen, initially all the energy is stored in the internal degrees of freedom (muscular potential energy), however as time goes, the flexion angle θ increases, thus the mechanical energy of the center of mass grows and the internal energy decreases. As the energy of the center of mass reaches its maximum, the reaction force vanishes and the body takes off. The subsequent dynamics of the jumper is governed by the center-of-mass energy fraction, that is, greater is it relative to the internal energy, more efficient will be the jump. Any improvement of E_G (that is, on the take-off velocity) requires to decrease the energy of internal motions. In the following Section 3.2.3, we study the variations of these ratios accordingly with the different possible mass distributions. Notice that the take-off condition (1), that is $\frac{dE_G}{dt} = 0$, provides θ_c, hence the take-off values for all energies.

Similarly, in Fig. 5, we plot $\hat{F}_N = \frac{F_N s}{T}$ vs θ for various initial flexion angles and knee torques. The computed reaction shows a generic behavior. Initially, the force of reaction increases up to a maximum value $F_N^{\max}$ at some angle $\theta^{\max}$, further it decreases up to its vanishing at take-off at the angle θ_c ($F_N(\theta_c) = 0$). Notice that if the initial angle is close to $\pi/2$, the maximal reaction force, $F_N^{\max}$, is larger. This is a consequence of the smallness of the take-off time, indeed, for $\theta \lesssim \pi/2$ the take-off time, t_c, is smaller, therefore the acceleration, $\sim V_G/t_c$ is larger, hence for the normal force (F_N). However, in this

[3] Notice that other re-scaled quantities may be considered, but the current choice appears to be the most adequate.

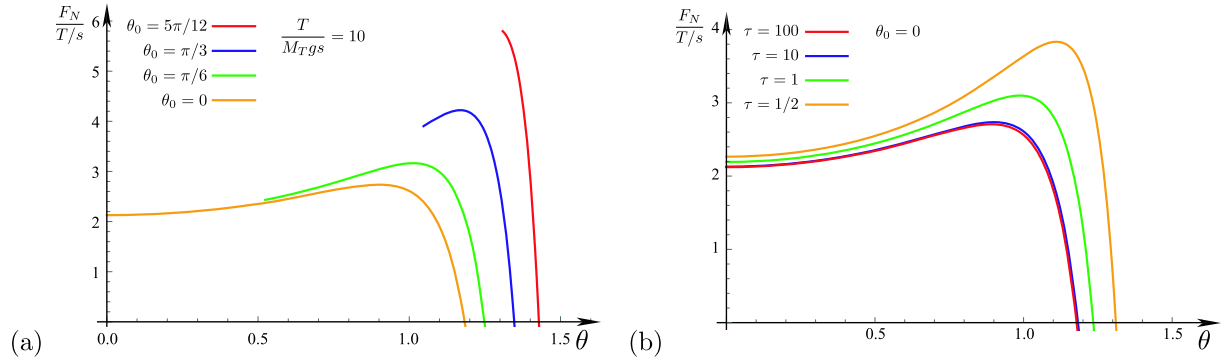

Fig. 5. Dimensionless reaction force as a function of the flexion angle θ for the two-segment model. (a) Plot of the reaction force $\hat{F}_N = \frac{F_N s}{T}$ vs θ for various initial flexion angles: $\theta_0 = \{0, \pi/6, \pi/3, 5\pi/12\}$, and for a dimensionless torque $\tau = \frac{T}{M_T gs} = 10$. (b) Plot of the reaction force $\hat{F}_N = \frac{F_N s}{T}$ vs θ for various dimensionless torques $\tau = \{1/2, 1, 10, 100\}$, for an initial flexion angle $\theta_0 = 0$. In the plot, we consider the two-segment model and the parameter values: $m_1/M_T = 0.7$, $m_2/M_T = 0.2$, and $m_3/M_T = 0.1$.

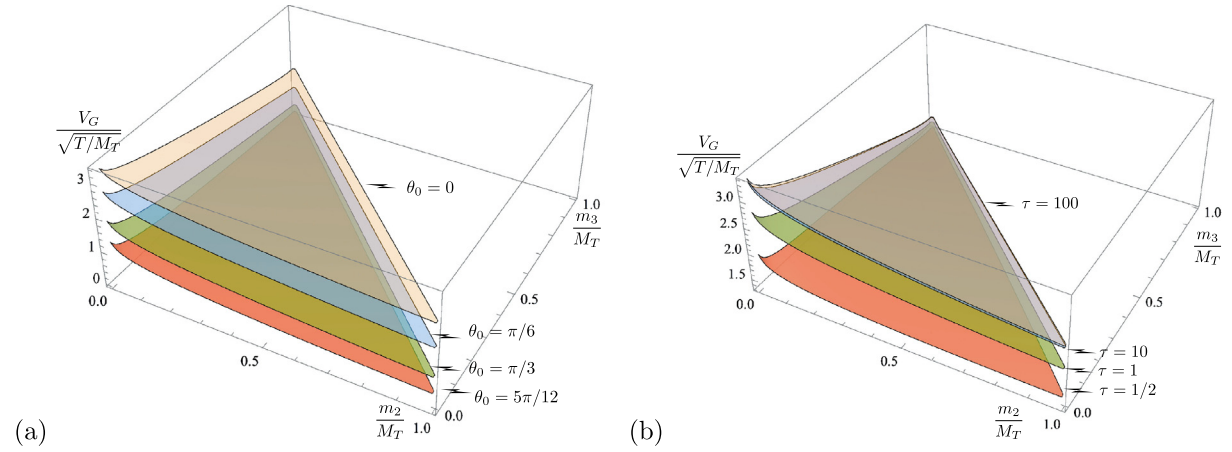

Fig. 6. Dimensionless take-off velocity $V_G/\sqrt{T/M_T}$ as a function of the mass distribution of the body and the extremities, for distinct conditions. (a) Jumping velocity for different initial flexion angle, namely for $\theta_0 \in \{0, \pi/6, \pi/3, 5\pi/12\}$ and for a torque given by $T/(M_T gs) = 64$. The maximum take-off speed arises for $\theta_0 = 0$ and for $m_2/M_T \to 0$ and $m_3/M_T \to 0$. (b) Jumping velocity for $\theta_0 = 0$ and for a distinct knee torque $T/(M_T gs) = \{1/2, 1, 10, 100\}$. We notice that, as $T/(M_T gs) \to \infty$, the take-off velocity reaches a well-defined limit, studied below.

case (*e.g.*, Fig. 5(a), for $\theta_0 = 5\pi/12$), the force just decreases from the initial value $F_N(\theta_0)$ up to when it vanishes at take-off. Fig. 5b shows the reaction force for $\theta_0 = 0$ and for various torques. As expected, initially the force of reaction increases up to a maximum, then it decreases, vanishing at take-off. The used scaling $\hat{F}_N = \frac{F_N s}{T}$ has the advantage that characterizes well the limit $\tau = T/(M_T gs) \to \infty$, a proof of that it emerges due to the almost successful overlap for the cases $\tau = 10$ and $\tau = 100$.

3.2.3. Determination of take-off velocity

Equation (11) together with $F_N = 0$ provide the take-off conditions (see Eq. (32) in 5.2). As mentioned, these conditions are solved numerically for the unknown variables θ_c. Once solving for θ_c, one replaces it into $\dot{\theta}_c$ together with the rest of the required parameters.

This can be done by employing the set of parameters (15) together with θ_0. The range of values is $\{m_2/M_T, m_3/M_T\} \in [0, 1]$ with the constraint $m_2/M_T + m_3/M_T \leq 1$. The initial flexion angle varies into the range $\theta_0 \in [0, \pi/2]$ and $\tau = T/(M_T gs) \in [0, \ldots\infty)$. The numerical computation of the take-off velocity for different values of the mass distribution is shown in Fig. 6. As it can be seen, the dimensionless velocity reaches its maximum at the corner where both m_2/M_T and $m_3/M_T \to 0$, and $m_1 \to M_T$.

This observation is verified by some insects, *e.g.*, the locusts and grasshoppers. For a *Schistocerca*, the legs are 17% of the body mass, while in some vertebrates, *e.g.*, humans or galagos, the legs are 30% (see Ref. [9]). We think that this leg design might be explained through an optimization process (for species in which jumping is the main locomotion mechanism). In other words, in this optimization process, the internal energy, which is useless after take-off, is decreased, localizing all the body mass near the center of mass.

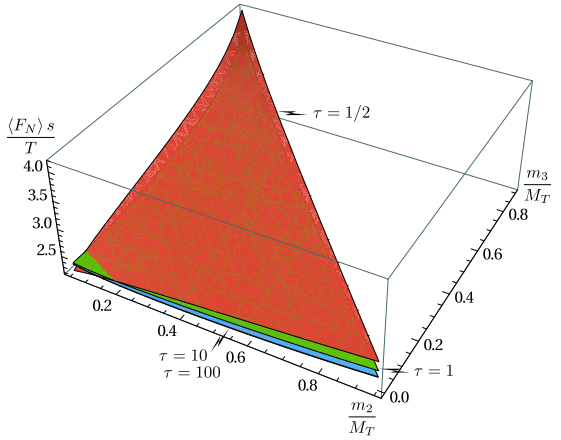

Fig. 7. Mean dimensionless reaction force $\langle F_N\rangle\, s/T$ as function of the mass distribution of the body and the extremities, for distinct conditions: dimensionless reaction force for $\theta_0 = 0$ and distinct knee torque $T/(M_T g s) = \{1/2, 1, 10, 100\}$. We notice that, as $T/(M_T g s) > 10$, the dimensionless reaction forces reach a well-defined limit studied below.

We notice that, in all cases, the dimensionless take-off velocity varies by a factor of 2 or 3. Therefore, a substantial change of configuration does not imply necessarily a significant increase in take-off velocity. More importantly, we conclude that $\hat{V}_G \lesssim 3.5$, thus $V_G \lesssim 3.5\sqrt{T/M_T}$, in agreement with the general bound condition (4). (Notice that $\Delta U_m = 2\pi T$, thus (4) coincides with $V_G \leq 2\sqrt{\pi T/M_T} \approx 3.5\sqrt{T/M_T}$.)

3.2.4. Determination of the reaction force

Similarly, we can compute the reaction force $F_N(\theta)$ for any flexion angle. The average reaction force reads:

$$\langle F_N\rangle = \frac{1}{t_c}\int_{\theta_0}^{t_c} F_N(t')\mathrm{d}t' = \frac{\int_{\theta_0}^{\theta_c} F_N(\theta)\,\frac{\mathrm{d}\theta}{\dot\theta}}{\int_{\theta_0}^{\theta_c}\frac{\mathrm{d}\theta}{\dot\theta}}$$

and it can be computed numerically for different parameter values of the model.

The numerical computations of the reaction force as a function of different values of mass distribution is shown in Fig. 7.

Because $\left\langle \hat{F}_N \right\rangle$ has a well-defined limit as $\tau \to \infty$ (see next Sect. 3.3), and because of the assumption $T \sim U_e M_T$, one gets $\left\langle \hat{F}_N \right\rangle = \frac{\langle F_N\rangle s}{U_e M_T} \equiv \frac{\langle F_N\rangle}{M_T g}\frac{gs}{U_e}$, which scales as a constant, thus $\langle F_N\rangle/(M_T g) \sim \frac{U_e}{gs}$, in agreement with the general results of Sects. 2.4 and Fig. 2.

3.3. Analytical results in the zero-g limit

The zero-g limit is a special case, because it limits the jumping performance. It is expected that gravity is always against jump because some energy must be used to move the center of mass. In this limit, muscular energy is used only in kinetic motions: the translation of the center of mass and the relative motion, which are useless for jumping performance. Therefore, the zero-g limit requires some attention.

In the special limit of zero gravity ($g \to 0$), that is, $\tau = \frac{T}{M_T g s} \to \infty$, one derives the normal force (13) as:

$$F_N = 2\delta_2 \frac{(a + b\cos^2\theta)\cos\theta - 2a(\theta - \theta_0)\sin\theta}{(a + b\cos^2\theta)^2} \tag{16}$$

Here we have used the short-hand notation used in Appendix 5.2, namely $a = \frac{1}{3}(m_2 + m_3)s^2$ and $b = 2(2m_1 + m_2)s^2$.

Take-off implies a condition for the angle that does not depend explicitly on T:

$$\frac{2a(\theta_c - \theta_0)}{a + b\cos^2\theta_c} = \cot\theta_c \tag{17}$$

In the same limit, after (11), the take-off angular speed $\dot\theta_c$ reads:

$$\dot\theta_c^2 = \frac{8T(\theta_c - \theta_0)}{a + b\cos^2\theta_c} \tag{18}$$

Therefore, the dimensionless take-off speed can be written as

$$\hat{V}_{\mathrm{G}} = \frac{V_{\mathrm{G}}}{\sqrt{T/M_{\mathrm{T}}}} = \delta_2 \sqrt{\frac{\cos^3\theta_{\mathrm{c}}}{aM_{\mathrm{T}}\sin\theta_{\mathrm{c}}}} \tag{19}$$

Though Eq. (17) is still a non-algebraic equation, it may be simplified for some special limits, which we discuss in what it follows. The cases of interest are those special limits in which the mass is concentrated on a particular part of the body. In the following we consider in detail three special limits.

3.3.1. The limit $m_1 \to M_{\mathrm{T}}$

In the limit $m_1 \to M_{\mathrm{T}}$ (all other masses vanish), after (9) and (10), we can write:

$$a = 0, \quad b = 4M_{\mathrm{T}}s^2, \quad \& \quad \delta_2 = 4M_{\mathrm{T}}s$$

Because this is a singular limit, we consider the asymptotic behavior as $a = \frac{1}{3}(M_{\mathrm{T}} - m_1)s^2 \to 0$. In this limit, Eq. (17) reads:

$$\frac{a}{2M_{\mathrm{T}}s^2}(\theta_{\mathrm{c}} - \theta_0) = \frac{\cos^3\theta_{\mathrm{c}}}{\sin\theta_{\mathrm{c}}} \tag{20}$$

Therefore, if $a \to 0$, one concludes that $\cos\theta_{\mathrm{c}} \to 0$, hence $\theta_{\mathrm{c}} \to \frac{\pi}{2}$. It is easy to see that the asymptotic behavior as $a \to 0$ is:

$$\theta_{\mathrm{c}} = \frac{\pi}{2} - \left(\frac{a(\pi - 2\theta_0)}{4s^2M_{\mathrm{T}}}\right)^{1/3} + \mathcal{O}(a^{2/3})$$

Moreover, evaluating the take-off velocity (19):

$$\hat{V}_{\mathrm{G}} = \frac{V_{\mathrm{G}}}{\sqrt{T/M_{\mathrm{T}}}} = 2\sqrt{\pi - 2\theta_0} + \mathcal{O}(a^{4/3}) \tag{21}$$

However this speed is bounded from above for the particular value $\theta_0 = 0$, hence

$$\hat{V}_{\mathrm{G}} \leq 2\sqrt{\pi} \approx 3.545\ldots$$

as the general bound (4). Performing a similar analysis for the normal force, it reads

$$F_{\mathrm{N}} \approx \frac{2T}{s\cos\theta}$$

The maximum reaction push-off force $F_{\mathrm{N}}^{\max} = F_{\mathrm{N}}(\theta^{\max})$ with $\theta^{\max}$ defined through $F'_{\mathrm{N}}(\theta^{\max}) = 0$ (see Fig. 4), reads, after some work [4]

$$\hat{F}_{\mathrm{N}}^{\max} = \frac{F_{\mathrm{N}}^{\max}s}{T} \approx \frac{3^{4/3}}{2}\frac{1}{((\pi - 2\theta_0)(1 - m_1/M_{\mathrm{T}}))^{1/3}} \tag{22}$$

Although the push-off force peak diverges as $m_1 \to M_{\mathrm{T}}$, the mean force,

$$\left\langle \hat{F}_{\mathrm{N}} \right\rangle = \frac{\langle F_{\mathrm{N}} \rangle s}{T} \approx \frac{\int_{\theta_0}^{\theta_{\mathrm{c}}} \frac{2}{\sqrt{\theta - \theta_0}}\mathrm{d}\theta}{\int_{\theta_0}^{\theta_{\mathrm{c}}} \frac{\cos\theta}{\sqrt{\theta - \theta_0}}\mathrm{d}\theta}$$

is finite. The integration may be written in terms of Fresnel functions; nevertheless, in the case of an initial flexion angle $\theta_0 = 0$, one has

$$\left\langle \hat{F}_{\mathrm{N}} \right\rangle = \left.\frac{\langle F_{\mathrm{N}} \rangle s}{T}\right|_{\theta_0 = 0} = 2.564$$

[4] In the limit $a \to 0$, the maximum force is located near $\pi/2$, looking for the same scaling one gets $\theta^{\max} \approx \frac{\pi}{2} - (\pi - 2\theta_0)^{1/3}\left(\frac{4a}{b}\right)^{1/3}$, therefore the final force takes the form (22).

3.3.2. The limit $m_2 \to M_T$

The limit $m_2 \to M_T$ (all other masses vanish) is regular, therefore, one has

$$a = \frac{1}{3} M_T s^2, \quad b = 2 M_T s^2, \quad \& \quad \delta_2 = 3 M_T s$$

Condition (17) is reduced to

$$\frac{2(\theta_c - \theta_0)}{1 + 6\cos^2\theta_c} = \cot\theta_c \tag{23}$$

leading to $\theta_c = 0.97590$ ($\theta_c = 55.9°$) for $\theta_0 = 0$. In this limit, the take-off speed, the maximum normal force and its average read

$$\hat{V}_G = \frac{V_G}{\sqrt{T/M_T}} = 1.69, \quad \hat{F}_N^{\max} = \left.\frac{F_N^{\max} s}{T}\right|_{\theta_0=0} = 2.58 \quad \& \quad \left\langle \hat{F}_N \right\rangle = \left.\frac{\langle F_N \rangle s}{T}\right|_{\theta_0=0} = 2.43$$

3.3.3. The limit $m_3 \to M_T$

In the limit $m_3 \to M_T$ (all other masses vanish), one has

$$a = \frac{1}{3} M_T s^2, \quad b = 0 \quad \& \quad \delta_2 = M_T s$$

In this case, the take-off condition (17) reads:

$$2(\theta_c - \theta_0) = \cot\theta_\infty$$

leading to $\theta_c = 0.65327$ ($\theta_c = 37.4°$) for $\theta_0 = 0$. In this case, one gets similar results as above

$$\hat{V}_G = \frac{V_G}{\sqrt{T/M_T}} = 1.69, \quad \hat{F}_N^{\max} = \left.\frac{F_N^{\max} s}{T}\right|_{\theta_0=0} = 6, \quad \& \quad \left\langle \hat{F}_N \right\rangle = \left.\frac{\langle F_N \rangle s}{T}\right|_{\theta_0=0} = 4.76$$

3.4. Discussion

In this subsection, we have presented the special limit of the zero-gravity jump. This limit is interesting because it allows us to compare the general case with the situation in which the muscular forces are more important than the gravity forces (the weight). That is, whenever $T/(M_T g s) \gg 1$. Qualitatively, we observe similar results than in both cases, indicating the minor role of gravity in the process of a self-propelled jump. As a sub-product, from an analytical point of view it has been computed exactly, in sections 3.3.1, 3.3.2 and 3.3.3, the main observables $\hat{V}_G$ and $\left\langle \hat{F}_N \right\rangle$ for some special configurations. The optimal take-off velocity is for $m_1 \to M_T$ and leads to $\hat{V}_G \leq 2\sqrt{\pi}$.

4. Concluding remarks and general discussion

Based on general mechanical conditions, we show that the jumping take-off occurs at the maximum value of the mechanical energy of the center of mass. Briefly, a jumper may increase its center of mass mechanical energy only if it is supported by some external force. As a consequence, to increase the kinetic energy before take-off, the body needs to increase the contact forces on the ground. Further, following an energy argument, the take-off velocity of the center of mass is bounded by the stored elastic energy per unit mass. The jumping velocity bound (4) eventually does not depend on the body mass, represented by the horizontal line in Fig. 1, because the elastic energy per unit mass should be an intrinsic feature characterizing bio-materials, accordingly with Borelli's law.

Moreover, our analysis could be useful for other self-propelled organisms like fungi [2] and plants [19,20] which display mechanisms for seed or spore dispersal, consistent with the current jump definition. In the same way, these results could be helpful to design artificial jumpers, focused on maximizing the amount of stored energy with a minimization of mass (density of energy) [21]. We emphasize that the limit velocity for living organisms is not the same as that of artificial jumpers, like for example, robots. Indeed, artificial jumpers are expected to have different amounts of stored energy per unit mass for jump, like chemical energy provided by batteries, therefore it is expected that these situations will manifest a different take-off velocity bound, *e.g.* Some studies [4] reports take-off velocities of some engines as large as 9 m/s.

At this stage, we cannot evaluate the nature of large variations on take-off velocity among species, readily seen in Fig. 1, for the same body mass. Probably, these variations are a consequence of the specific design. In a future publication [22], we will consider a more realistic assumption, whereas the muscular energy comes only from the extremities (because most of the muscular energy comes from the muscular mass of the thigh and the limb and not from the full body mass).

On the other hand, under these assumptions, it is found that the mean reaction force before take-off scales as (7) for a large number of different organisms as shown in Fig. 2.

Finally, we illustrate the general results in the frame of Alexander's model, which can be exactly solved in some special limits.

We end this paper commenting on a recent research performed with mantises [5]. In this study, it was observed (see Fig. 1) a possible scaling regarding the dependence of take-off velocity and size of mantis. Roughly, the scaling is consistent with a constant power per unit mass. More precisely, if $\mathcal{P}$ is the muscular power released per unit mass, then the take-off velocity is consistent, by dimensional analysis, with:

$$V_{\mathrm{G}} \sim (\mathcal{P}s)^{1/3}$$

Because the body size scales as $s \sim M_{\mathrm{T}}^{1/3}$, based on his results, Sutton et al. conjecture the scaling

$$V_{\mathrm{G}} \sim M_{\mathrm{T}}^{1/9}$$

This law can be extrapolated from the respective data (black triangles) plotted in Fig. 1. Though a constant energy per mass and a constant power per mass processes appear to be both qualitatively and quantitatively different, it must be pointed out that the mantises' take-off velocity is still consistent with a limiting speed derived in this current work. Note that both behaviors coincide for a mass of the order of 10^3 kg, validating the idea of a constant energy per unit mass limiting speed, for all those species such that $M_{\mathrm{T}} < 10^3$ kg.

5. Appendices

5.1. Lagrangian formulation of the two-segment model

The kinetic energy of the model (see Fig. 3) reads

$$K = \frac{m_1 v_1^2}{2} + \frac{m_2 v_2^2}{2} + \frac{m_3 v_3^2}{2} + \frac{I_2 \dot{\theta}^2}{2} + \frac{I_3 \dot{\theta}^2}{2} \tag{24}$$

where v_1^2, v_2^2, and v_3^2 are the squared speeds of the center of mass of the trunk and of the second and third leg segments. Moreover, $I_2 = \frac{m_2 s^2}{24}$ and $I_3 = \frac{m_3 s^2}{24}$ are the moments of inertia of each thigh and each limb, respectively, and $\dot{\theta}$ is the angular velocity of the leg parts. Ultimately, all speeds are proportional to $\dot{\theta}$. Therefore, the total kinetic energy reads

$$K[\theta, \dot{\theta}] = \frac{1}{2} I_2(\theta) \dot{\theta}^2 \tag{25}$$

where we define $I_2(\theta)$ by Eq. (9). The potential energy includes the gravitational energy:

$$U_{\mathrm{G}} = \frac{\delta_2}{2} g \sin\theta \tag{26}$$

where δ_2 is defined by Eq. (10), and the stored energy by the muscle knees:

$$U_{\mathrm{m}} = 4T\left(\frac{\pi}{2} - \theta\right) \geq 0 \tag{27}$$

Notice that we define the zero muscular energy by the energy at a non-elongated configuration. Therefore, the total potential energy reads

$$U(\theta) = \frac{\delta_2}{2} g \sin\theta - 4T\left(\frac{\pi}{2} - \theta\right) \tag{28}$$

5.2. Lagrangian formalism

In this appendix, we review the general Lagrangian formalism as applied to this model. The equation of motion of the jumper can be obtained directly from a Lagrangian function. The Lagrangian of the jumper reads:

$$\mathcal{L} = \frac{1}{2}\left(a + b\cos^2\theta\right)\dot{\theta}^2 - \frac{\delta}{2} g \sin\theta + 4T\left(\theta - \frac{\pi}{2}\right) \tag{29}$$

where a and b are parameters for a two-segment model

$$a = \frac{1}{3}(m_2 + m_3)s^2, \quad \& \quad b = 2(2m_1 + m_2)s^2$$

The Euler–Lagrange equations for the Lagrangian (29) gives the ordinary differential equation (ODE),

$$\ddot{\theta} = \frac{\left[b \sin\theta \cos\theta \dot{\theta}^2 - \frac{\delta_2}{2} g \cos\theta + 4T\right]}{\left(a + b\cos^2\theta\right)} \tag{30}$$

which was solved numerically by Alexander [9]. In principle, this ODE solves the problem; however, the variational approach provides us with a conserved quantity, which appears to be the energy (8) and which is settled *a priori* by the initial configuration of the jump:

$$E = \frac{1}{2} I(\theta)\dot{\theta}^2 + g\delta \sin\theta - 8\theta = g\delta \sin\theta_0 - 8\theta_0$$

hence, one recovers the general expression for $\dot{\theta}^2$ as in Eq. (11).

The normal force defined by Eq. (13) can be expressed using (8) and (30) by a function that depends only on the angular variable θ:

$$\begin{aligned} F_N &= M_T g + \frac{\delta_2}{2}(\cos\theta\ddot{\theta} - \sin\theta\dot{\theta}^2), \\ &= \frac{1}{4(a + b\cos^2\theta)}\left[4aM_T g + 8T\delta\cos\theta + (4M_T b - \delta^2)g\cos^2\theta - \frac{16aT\delta(\theta - \theta_0)\sin\theta}{(a + b\cos^2\theta)}\right] \end{aligned} \tag{31}$$

The take-off condition appears, after imposing $F_N = 0$:

$$4aM_T g + 8T\delta\cos\theta + (4M_T b - \delta^2)g\cos^2\theta = \frac{16aT\delta(\theta - \theta_0)\sin\theta}{(a + b\cos^2\theta)} \tag{32}$$

This non-algebraic equation provides the take-off angle θ_c, and the take-off angular speed $\dot{\theta}_c$ (equation (11)). The reader may directly notice that this condition arises also from $\mathcal{P}_G = \frac{dE_G}{dt} \equiv 0$.

Finally, replacing these values into the take-off expression for the center of mass velocity (12), one obtains (14).

Acknowledgements

MCJ thanks her CONICYT doctoral fellowship No. 21140279. The authors acknowledge Fernando Mora for his help.

References

[1] G. Borelli, De motu animalium (1680–1681), Bernabo, Rome, 1680.
[2] X. Noblin, S. Yang, J. Dumais, Surface tension propulsion of fungal spores, J. Exp. Biol. 212 (2009) 2835–2843.
[3] W.J. Garrison, G.L. Miller, R. Raspet, Ballistic seed projection in two herbaceous species, Am. J. Bot. 87 (2000) 1257–1264.
[4] M. Ilton, M.S. Bhamla, X. Ma, S.M. Cox, L.L. Fitchett, Y. Kim, J-s. Koh, D. Krishnamurthy, C.-Y. Kuo, F.Z. Temel, et al., The principles of cascading power limits in small, fast biological and engineered systems, Science 360 (2018) eaao1082.
[5] G.P. Sutton, M. Doroshenko, D.A. Cullen, M. Burrows, Take-off speed in jumping mantises depends on body size and a power-limited mechanism, J. Exp. Biol. 219 (2016) 2127–2136.
[6] F.C. Anderson, M.G. Pandy, A dynamic optimization solution for vertical jumping in three dimensions, Comput. Methods Biomech. Biomed. Eng. 2 (1999) 201–231.
[7] M.F. Bobbert, Effects of isometric scaling on vertical jumping performance, PLoS ONE 8 (2013) e71209.
[8] J.D. Wong, M.F. Bobbert, A.J. van Soest, P.L. Gribble, D.A. Kistemaker, Optimizing the distribution of leg muscles for vertical jumping, PLoS ONE 11 (2016) e0150019.
[9] R.M. Alexander, Leg design and jumping technique for humans, other vertebrates and insects, Philos. Trans. R. Soc. Lond. B, Biol. Sci. 347 (1995) 235–248.
[10] M.N. Scholz, M.F. Bobbert, A. Knoek van Soest, Scaling and jumping: gravity loses grip on small jumpers, J. Theor. Biol. 240 (2006) 554–561.
[11] J. Aguilar, A. Lesov, K. Wiesenfeld, D.I. Goldman, Liftoff dynamics in a simple jumping robot, Phys. Rev. Lett. 109 (2012) 174301.
[12] R.S. James, C.A. Navas, A. Herrel, How important are skeletal muscle mechanics in setting limits on jumping performance?, J. Exp. Biol. 210 (2007) 923–933.
[13] J.M. Gabriel, The effect of animal design on jumping performance, J. Zool. 204 (1984) 533–539.
[14] S. Vogel, Living in a physical world III. Getting up to speed, J. Biosci. 30 (2005) 303.
[15] W. Gronenberg, Fast actions in small animals: springs and click mechanisms, J. Comp. Physiol. A 178 (1996) 727–734.
[16] T.J. Roberts, R.L. Marsh, Probing the limits to muscle-powered accelerations: lessons from jumping bullfrogs, J. Exp. Biol. 206 (2003) 2567–2580.
[17] H.C. Astley, T.J. Roberts, Evidence for a vertebrate catapult: elastic energy storage in the plantaris tendon during frog jumping, Biol. Lett. 8 (2012) 386–389.
[18] P. Aerts, Vertical jumping in Galago senegalensis: the quest for an obligate mechanical power amplifier, Philos. Trans. R. Soc. Lond. B, Biol. Sci. 353 (1998) 1607–1620.
[19] D. Evangelista, S. Hotton, J. Dumais, The mechanics of explosive dispersal and self-burial in the seeds of the filaree, Erodium cicutarium (Geraniaceae), J. Exp. Biol. 214 (2011) 521–529.
[20] C.C. Nicholson, J.W. Bales, J.E. Palmer-Fortune, R.G. Nicholson, Darwin's bee-trap: the kinetics of Catasetum, a New World orchid, Plant Signal. Behav. 3 (2008) 19–23.
[21] R. Armour, K. Paskins, A. Bowyer, J. Vincent, W. Megill, Jumping robots: a biomimetic solution to locomotion across rough terrain, Bioinspir. Biomim. 2 (2007) S65, S82.
[22] M. Jarur, S. Rica, J. Dumais, 2019, in preparation.